

Published in final edited form as:

Radiat Res. 2013 May ; 179(5): 549–556. doi:10.1667/RR3026.1.

Selective Inhibition of Microglia-Mediated Neuroinflammation Mitigates Radiation-Induced Cognitive Impairment

Kenneth A Jenrow^{a,1}, Stephen L. Brown^b, Karen Lapanowski^b, Hoda Naei^b, Andrew Kolozsvary^b, and Jae Ho Kim^b

^aDepartment of Neurosurgery, Henry Ford Hospital, Detroit, Michigan

^bDepartment of Radiation Oncology, Henry Ford Hospital, Detroit, Michigan

Abstract

Cognitive impairment precipitated by irradiation of normal brain tissue is commonly associated with radiation therapy for treatment of brain cancer, and typically manifests more than 6 months after radiation exposure. The risks of cognitive impairment are of particular concern for an increasing number of long-term cancer survivors. There is presently no effective means of preventing or mitigating this debilitating condition. Neuroinflammation mediated by activated microglial cytokines has been implicated in the pathogenesis of radiation-induced cognitive impairment in animal models, including the disruption of neurogenesis and activity-induced gene expression in the hippocampus. These pathologies evolve rapidly and are associated with relatively subtle cognitive impairment at 2 months postirradiation. However, recent reports suggest that more profound cognitive impairment develops at later post-irradiation time points, perhaps reflecting a gradual loss of responsiveness within the hippocampus by the disruption of neurogenesis. We hypothesized that inhibiting neuroinflammation using MW01-2-151SRM (MW-151), a selective inhibitor of proinflammatory cytokine production, might mitigate these deleterious radiation effects by preserving/restoring hippocampal neurogenesis. MW-151 therapy was initiated 24 h after 10 Gy whole-brain irradiation (WBI) administered as a single fraction and maintained for 28 days thereafter. Proinflammatory activated microglia in the dentate gyrus were assayed at 2 and 9 months post-WBI. Cell proliferation and neurogenesis in the dentate gyrus were assayed at 2 months post-WBI, whereas novel object recognition and long-term potentiation were assayed at 6 and 9 months post-WBI, respectively. MW-151 mitigated radiation-induced neuroinflammation at both early and late time points post-WBI, selectively mitigated the deleterious effects of irradiation on hippocampal neurogenesis, and potently mitigated radiation-induced deficits of novel object recognition consolidation and of long-term potentiation induction and maintenance. Our results suggest that transient administration of MW-151 is sufficient to partially preserve/restore neurogenesis within the subgranular zone and to maintain the functional integrity of the dentate gyrus long after MW-151 therapy withdrawal.

INTRODUCTION

Patients receiving large-volume or whole-brain irradiation (WBI) for treatment of primary or metastatic brain tumors are at significant risk for the development of late radiation injury to normal brain tissue that can manifest as mild-to-severe cognitive impairment (1–3). Such cognitive impairment has a diverse character, but typically includes deficits in hippocampal-dependent functions involving learning and memory and spatial information processing (4).

The risk of radiation-induced cognitive impairment is particularly relevant for patients with long survival expectancies, since it typically requires more than 6 months to manifest (5, 6). There are currently no preventive or mitigating strategies for successfully treating cognitive impairment resulting from late irradiation brain injury.

Several animal studies have confirmed the importance of hippocampal injury in the evolution of radiation-induced cognitive impairment and provide compelling evidence that such effects can be reliably produced by radiation doses that do not cause overt tissue destruction (7–12). Neuroinflammation mediated by activated microglial cytokines has been consistently implicated in the pathogenesis of radiation-induced cognitive impairment in these animal models where it impairs both neurogenesis and the behaviorally-induced expression of immediate-early genes (IEGs) in the hippocampus (7–9, 11–13). These pathologies evolve rapidly after radiation exposure and are associated with relatively subtle cognitive impairment between 4–8 weeks postirradiation, when many of these studies are terminated. However, more profound cognitive impairment of recognition memory has recently been reported to manifest at 6 and 9 months postirradiation, suggesting that the pathogenesis initiated by neuroinflammation may continue to evolve and mirror the kinetics and severity of cognitive impairment associated with clinical late irradiation effects (14, 15).

Hippocampal neurogenesis occurs exclusively within the dentate gyrus, where resident neural progenitors proliferate within a specialized niche called the subgranular zone (SGZ) (16). Newborn neurons migrate from the SGZ into the adjacent granule cell layer where they may differentiate to become mature granule cell neurons. The survival of these immature neurons is activity-dependent and is determined between 11 and 16 days post-mitosis during the early stages of synapse formation (17–19). Surviving neurons exert a hyperexcitable influence on the hippocampal network during a prolonged period of synaptic integration that lasts approximately 120 days post-mitosis and persists until approximately 160 days post-mitosis when these cells reach physiological maturity (17, 20–22). WBI doses of 10 Gy are sufficient to impair neurogenesis within the rat hippocampus, reflecting both a rapid depletion of neuronal progenitors mediated by apoptosis and mitotic catastrophe and a more gradual disruption of neurogenic signaling mediated by proinflammatory microglial cytokines (2, 5). This loss of neurogenic potential compromises both acute activity-dependent increases in proliferation and survival among newly differentiated neurons and the continual influx of immature and hyperexcitable neurons into the hippocampal network. Thus, the deleterious effects of WBI and impaired neurogenesis on the hippocampal network may continue to evolve over several months as preexisting immature neurons complete their anatomical and physiological maturation.

Here we present the results of our initial attempt to mitigate the effects of radiation-induced neuroinflammation on hippocampal neurogenesis using MW01-2-151SRM (MW-151), a selective inhibitor of proinflammatory microglial cytokine production. MW-151 is a water soluble, nontoxic, bioavailable, central nervous system-penetrant compound that has previously been shown to mitigate proinflammatory cytokine production, glial activation and inflammation within the rat hippocampus. MW-151 has also been shown to prevent associated deficits in cognitive function when administered after status epilepticus (23), traumatic brain injury (24) and during the progression of Alzheimer's disease (25). In these animal models, MW-151 significantly attenuated trauma-induced increases in IL-1 β , IL-6, TNF- α and CCL2, and normalized synaptic function (23–25). Our results indicate that MW-151, when administered for 28 days after 10 Gy WBI, similarly reduces neuroinflammation and mitigates the deleterious effects of 10 Gy WBI on neurogenesis at 2 months postirradiation and radiation-induced deficits of novel object recognition (NOR) consolidation and long-term potentiation (LTP) induction and maintenance when assayed at 6 and 9 months postirradiation, respectively.

METHODS

Experimental Design

Adult male Fischer 344 rats (Charles River Laboratories, Inc., Wilmington, MA) weighing between 200–240 g were used in all experiments. All animal procedures were performed with approved protocols and in accordance with published recommendations for the proper use and care of laboratory animals. A total of 36 rats were randomly assigned to separate treatment groups in a 2 × 2 factorial design. Whole-brain irradiation was administered at doses of 0 or 10 Gy. Mitigating therapy with MW-151 or equivalent volumes of saline (sham) was initiated 24 h post-WBI and maintained for 28 days. The resultant groups were 0 Gy sham ($n = 10$), 0 Gy MW-151 ($n = 6$), 10 Gy sham ($n = 10$) and 10 Gy MW-151 ($n = 10$). Half of the rats in each group were sacrificed at 2 months post-WBI, with the other half sacrificed at 9 months post-WBI. Progenitor proliferation and neurogenesis were assayed at 2 months post-WBI, and neuroinflammation was assayed at 2 and 9 months post-WBI. NOR and LTP were assayed in the same animals at 6 and 9 months, respectively.

Whole-Brain Irradiation

WBI at 10 Gy was administered with a dedicated self-shielded 5000Ci ^{137}Cs irradiator (Mark I, Model 68, J.L. Shepherd, San Fernando, CA), with a primary collimator used to create a 2 × 30 cm rectangular dose field. The measured dose rate at the time of irradiation was approximately 3.2 Gy/min. Under ketamine (60 mg/kg) and xylazine (6 mg/kg) anesthesia, rats were positioned horizontally with their heads at the midpoint of this field (centered 15 cm above the base and 6 cm forward of the collimator face) such that the radioactive source was lateral to the midline with the 2 cm dose field dimension encompassing the anterior-posterior extent of the brain. Secondary lead shielding (1 cm thick) was used to limit radiation exposure to structures outside the brain, including the jaw, pharynx, nose and eyes. To compensate for the effects of tissue attenuation, the prescribed radiation dose was administered bilaterally in two consecutive 5 Gy dose fractions. Rats receiving 0 Gy WBI were treated in an identical manner, but were not exposed to the radioactive source (26, 27).

Mitigating Therapy

MW-151 was obtained from Transition Therapeutics by a Material Transfer Agreement. The compound was dissolved in sterile saline at a concentration of 20 mg/ml. Mitigating therapy was initiated 24 h post-WBI and was continued for 28 days post-WBI by daily injection (5 mg/kg/day, i.p.) (23–25). Sham therapy was administered in an identical manner by injecting equivalent volumes of saline. After therapy was withdrawn, rats remained in their home cages until sacrifice.

Immunofluorescence

Immunofluorescence assays for cell proliferation and neurogenesis were performed at 2 months and for neuroinflammation at 2 and 9 months post-WBI. Rats were sacrificed by transcardial perfusion with saline (300 ml) followed by 10% neutral buffered formalin (300 ml) while under deep pentobarbital anesthesia (50 mg/kg). Brains were removed and post-fixed overnight at 4°C in 10% neutral buffered formalin, coronally sectioned into 2 mm blocks using a rat brain matrix and processed for paraffin embedding. Coronal sections (5 μm) were cut from the region 3.3–4.0 mm caudal to bregma, encompassing the anterior region of the rat hippocampus. One of these sections was stained with hematoxylin and eosin (H&E) for routine histological assessment. Cell proliferation and neurogenesis were assayed in multiple serial sections within this range by processing for double-label immunofluorescence staining for Ki67 (RB1510, 1/100, Lab Vision Thermo) and double

cortin (DCX) (SC8060, 1/100, Santa Cruz), respectively. Ki67 protein is expressed by multiple cell types and is indicative of active or recently completed cell division (28). DCX protein is expressed exclusively by newly differentiated neurons and is indicative of neurogenesis proper (29). Counts of Ki67⁺ and DCX⁺ cells within the dentate gyrus were performed in multiple sections for each rat by an individual naïve to the experimental conditions. Counting was performed bilaterally and was confined to the subgranular zone (SGZ) for Ki67 and to the SGZ and adjacent dentate granule cell layer for DCX. Proliferating Ki67⁺ cells within the SGZ were counted if this protein was expressed in the nucleus. Also, newly differentiated DCX⁺ neurons within the SGZ or granule cell layer were counted if this protein was expressed in the cytoplasm. As reported previously, cells expressing these proteins were commonly found in clusters within the SGZ where the identification of individual cells often required adjusting the focal plane of the microscope to facilitate the identification of cellular boundaries (16). Neuroinflammation was evaluated in multiple sections within this range by processing for single-label immunofluorescence staining for OX-6/ CD74 (SC53062, 1/50, Santa Cruz). OX-6 protein is expressed exclusively by activated microglia and is indicative of a proinflammatory level of activation among these cells (30). Counts of OX-6⁺ cells were performed in the entire dentate gyrus, including all subfields of the granule cell layer and the hilus. Volumes of these regions, used to calculate cell densities, were determined by measuring the respective areas in which the counts were obtained and were multiplied by section thickness.

Novel Object Recognition

NOR consolidation was selected as our behavioral assay due to its relative simplicity and the fact that others have previously reported NOR deficits after comparable doses of whole-brain irradiation. There is an ongoing debate regarding whether or not the hippocampus is required for NOR (42). However, Jessberger *et al.* (38) demonstrated conclusively that deficits in NOR consolidation manifest after selective impairment of hippocampal neurogenesis. Consolidation of NOR was assayed at 6 months post-WBI using established protocols (31). Rats were handled twice per day for 4 days, followed by a 3-day rest period prior to beginning experiments. Rats were habituated to the arena in the absence of objects for 2 ×, 5 min a day, for 3 days. Acquisition of “familiar” objects was conducted 24 h after the last habituation session. Two objects (F₁ and F₂) identical in size, shape and color, were placed in the rear corners of the arena and the rats were allowed to explore them for two 10-min sessions with a 5-min interval in between. Retention/consolidation was assayed 24 h after completing acquisition. Rats were placed in the arena for a single 10-min session with two new objects: one familiar (F), identical in every respect to the objects used during acquisition, and the other a novel object (N), which the rats had not previously encountered. Exploration times for the familiar and the novel objects were recorded (t_F and t_N , respectively), where exploration was operationally defined as the rat having both forelimbs within a circle extending ~5 cm beyond the periphery of the object in all directions, with the head oriented toward the object with vibrissae moving. These were used to calculate the discrimination index ($DI = t_N - t_F$), defined as the difference between the exploration times for F and N during the retention phase, and the discrimination ratio [$DR = DI/(t_N + t_F)$], defined as the ratio between DI and the sum of the exploration times for F and N.

Long-Term Potentiation

LTP of synaptic responses in the dentate gyrus induced by electrical stimulation of the perforant path was assayed at 9 months post-WBI using established protocols (32, 33). Stainless steel microelectrodes were positioned stereotactically relative to bregma in the dentate gyrus (AP: -3.6 mm, ML: 1.9 mm, monopolar) and perforant pathway (AP: -7.3 mm, ML: 3.8 mm, bipolar), with electrode depths set relative to the cortical surface at -3.0 mm and -2.5 mm, respectively. Biphasic constant current stimulation of the perforant path

was administered using a Grass S88 Dual Channel Square Pulse Stimulator configured with two Grass PSIU6 Photoelectric Stimulus Isolation Units. Excitatory post-synaptic potentials (EPSP) and population spikes produced in the dentate gyrus were amplified ($\times 100$) and band-pass filtered (1 Hz–10 kHz) using a Grass P55 AC Preamplifier, digitized using an Axon Instruments 1322A A/D Converter (10 KHz sampling frequency) and recorded for analysis offline. Input output (IO) functions were acquired before initiating LTP measurements by delivering biphasic test pulses (0.8 ms pulse width) to the perforant pathway at 10 s intervals. Stimulus intensity was increased incrementally from 20–1,500 μA , with 5 test pulses delivered at each increment. The IO function was used to determine the test pulse current used for assessing LTP, which was selected as the current producing population spike amplitudes approximately 50% of the maximum produced by a 1,500 μA test pulse. Test pulses were delivered at this amplitude at 30 s intervals for 10 min pre-LTP to establish the baseline response characteristics, and for 90 min post-LTP to monitor the induction and maintenance of synaptic potentiation. LTP was induced by delivering three biphasic pulse trains at 1,500 μA , with a 250 Hz intratrain frequency, a 200 ms train duration, and a 30 s intertrain interval. EPSP slopes and population spike amplitudes were averaged at 50 s intervals for each stimulus intensity for the pre- and post-LTP IO functions, and at 150 s intervals for the pre- and post-LTP measurements.

Sequencing of Assays

Neurogenesis was only assayed in the 2 month sacrifice group because the rate of hippocampal neurogenesis is known to decline with age, making it difficult to resolve the deleterious effects of irradiation in the 9 month sacrifice group. LTP was only performed as a terminal assay in the 9 month sacrifice group because LTP is known to effect the rate of hippocampal neurogenesis, and would likely have confounded the neurogenesis results in the 2 month sacrifice group. NOR and LTP were not assayed coincidentally in the 9 month sacrifice group because each of these assays can exert a prolonged influence on synaptic plasticity. NOR and LTP assays were therefore performed singly, separated by a 3 month interval, with LTP as the terminal assay. Thus, only OX-6⁺ microglial density within the dentate gyrus was assayed in both the 2 and 9 month sacrifice groups.

Analysis

For statistical analyses, rats were enrolled into one of 2 factor combination groups with factors of radiation dose (Gy) of (0, 10) and MW-151 treatment (yes, no). However, for all measures there was no distinction between 0 Gy treatment groups with or without MW-151 treatment. These groups were therefore combined to form a single control group for further analysis. Analyses for cell proliferation and neurogenesis were performed using the average densities of Ki67⁺ and DCX⁺ cells, respectively. These were compared using one-way analysis of variance (ANOVA) to test whether there was a decrease in proliferation/neurogenesis as a function of radiation dose and whether MW-151 was capable of mitigating the effects of radiation on proliferation/neurogenesis. Analysis for NOR was performed using average discrimination ratios (DR). These were compared using one-way ANOVA to test whether consolidation of novel object recognition was affected by radiation dose, and whether MW-151 mitigated the effects of WBI. Analysis for neuroinflammation was performed using the average cell densities of OX-6⁺ microglia at both sacrifice times (2 and 9 months postirradiation). These were compared at each time point using one-way ANOVA to test whether OX-6⁺ cell densities were affected by radiation dose and whether MW-151 mitigated the effects of WBI. Analyses of LTP induction/maintenance were performed using averages of the EPSP slopes during successive 2.5 min intervals spanning 10 min pre- and 90 min post-LTP induction. Repeated measures ANOVA was used to test whether the induction/ maintenance of LTP was affected by WBI, and whether MW-151 mitigated the effects of WBI. When these analyses indicated significance at the 0.05 level, Student-

Newman-Keuls tests were used to determine which conditions were significantly different from each other. All analyses were performed using SAS software (SAS Institute, Cary, NC).

RESULTS

MW-151 Mitigates WBI-Induced Deficits in Neurogenesis

Effects of MW-151 therapy on measures of cell proliferation (Ki67) and neurogenesis (DCX) within the dentate gyrus were assayed 2 months post-WBI, approximately 1 month after therapy withdrawal. Since MW-151 therapy had no effect on Ki67⁺ or DCX⁺ cell densities within the dentate gyrus among unirradiated controls, the 0 Gy sham and 0 Gy MW-151 groups were combined to form a single control group. Mean Ki67⁺ and DCX⁺ cell densities for controls were 9,259 ($\pm 1,477$) and 9,653 (± 831) cells/mm³, respectively. Relative to controls, mean Ki67⁺ and DCX⁺ cell densities in the 10 Gy group were significantly reduced ($P < 0.01$) to 4,975 (± 741) and 1,375 (± 535) cells/mm³, respectively. The deleterious effects of 10 Gy WBI on neurogenesis in the 10 Gy group were significantly mitigated ($P < 0.01$) in the 10 Gy MW-151 group, as evidenced by a significant ($P < 0.01$) increase in the mean DCX⁺ cell density to 4,702 (± 622) cells/mm³. However, MW-151 therapy did not mitigate the deleterious effects of 10 Gy WBI on cell proliferation, since the mean Ki67⁺ cell density of 4,884 (± 843) cells/mm³ was not significantly increased ($P > 0.5$) relative to the 10 Gy group (Fig. 1).

MW-151 Mitigates WBI-Induced Deficits in NOR Consolidation

Effects of MW-151 therapy on the consolidation of novel object recognition (NOR) were assayed 6 months post-WBI and 5 months after therapy withdrawal. Since MW-151 therapy had no effect on the DR among unirradiated controls, the 0 Gy sham and 0 Gy MW-151 groups were combined to form a single control group. The mean DR for controls was 68.76% ($\pm 11.30\%$), reflecting a clear and statistically significant ($P < 0.01$) preference to explore the novel object (Fig. 2). Relative to controls, the preference to explore the novel object was significantly reduced ($P < 0.01$) in the 10 Gy group, resulting in a DR of 21.71% ($\pm 10.86\%$). The deleterious effects of 10 Gy WBI on NOR memory were significantly mitigated in the 10 Gy MW-151 group, resulting in a DR of 77.43% ($\pm 6.37\%$) (Fig. 2).

MW-151 Mitigates WBI-Induced Deficits in LTP Induction and Maintenance

Effects of MW-151 therapy on LTP induction and maintenance over 90 min were assayed 9 months post-WBI and 8 months after therapy withdrawal. Since MW-151 therapy had no effect on LTP among unirradiated controls, the 0 Gy sham and 0 Gy MW-151 groups were combined to form a single control group (Fig. 3). Relative to baseline values established immediately prior to LTP induction, the mean percentage change in the EPSP slope for controls was 151.33% ($\pm 2.86\%$) during the first 150 s post-LTP and 127.89% ($\pm 3.40\%$) at 90 min post-LTP. Relative to controls, LTP induction and maintenance were significantly impaired ($P < 0.03$) in the 10 Gy group such that the corresponding changes in the EPSP slope were 136.90% ($\pm 3.86\%$) and 112.84% ($\pm 5.04\%$), respectively. These deleterious effects of 10 Gy WBI were significantly mitigated ($P < 0.03$) in the 10 Gy MW-151 group such that the corresponding changes in EPSP slope were 150.11% ($\pm 6.07\%$) and 123.71% ($\pm 3.71\%$), respectively (Fig. 3).

MW-151 Mitigates WBI-Induced Neuroinflammation

The deleterious effects of 10 Gy WBI and the mitigating effects of MW-151 in this context were correlated with levels of chronic neuroinflammation, assessed by quantifying densities of OX-6⁺ microglia within the dentate gyrus at 2 and 9 months post-WBI. Since MW-151

therapy had no effect on mean OX-6⁺ cell densities among unirradiated controls, the 0 Gy sham and 0 Gy MW-151 groups were combined to form a single control group. Mean OX-6⁺ cell densities for controls were 73 (\pm 51) and 121 (\pm 24) cells/mm³, respectively. Relative to controls, mean OX-6⁺ cell densities were significantly increased ($P < 0.01$) in the 10 Gy group to 1,966 (\pm 218) and 1,493 (\pm 270) cells/mm³, respectively. The proinflammatory effects of 10 Gy WBI were mitigated in the 10 Gy MW-151 group, where mean OX-6⁺ cell densities were significantly reduced ($P < 0.01$) to 849 (\pm 350) and 437 (\pm 119) cells/mm³, respectively (Fig. 4).

DISCUSSION

The mitigating effects of MW-151 with respect to hippocampal neurogenesis are consistent with previous reports demonstrating that reducing neuroinflammation helps to preserve or restore the integrity of neurogenic signaling within the dentate gyrus. Radiation-induced neuroinflammation disrupts microvascular niches within the SGZ that are required for neurogenic signaling (7–9). The compromise of this microenvironment causes the majority of surviving progenitors to adopt glial rather than neuronal fates (8). Since the majority of radiation-induced apoptosis among progenitors within the SGZ occurs within 24 h postirradiation and prior to the initiation of mitigating therapy, it is perhaps not surprising that they were similarly depleted in both the 10 Gy and 10 Gy MW-151 groups. However, the reduction of neuroinflammation by MW-151 was associated with a larger proportion of the surviving progenitors in the 10 Gy MW-151 group adopting neuronal fates (7, 8), presumably reflecting an improved neurogenic signaling microenvironment. The persistence of these mitigating effects after the withdrawal of MW-151 therapy suggests that inhibiting radiation-induced neuroinflammation for 28 days is sufficient to affect a sustained benefit in this context.

The profound functional deficits observed at later post-irradiation time points suggest a substantial disruption of learning and memory processes associated with increased neuroinflammation and/or impaired hippocampal neurogenesis. Both the timing and severity of these functional deficits are consistent with radiation-induced cognitive impairment observed clinically (5, 6). The dramatic mitigating effects produced by MW-151 in this context may be facilitated by improved neurogenesis and the sustained influence of immature and hyperexcitable granule cell neurons upon the hippocampal network. Neurogenesis-derived immature granule cell neurons possess unique synaptic characteristics that facilitate the induction of LTP relative to mature neurons under identical conditions (34, 35). These cells also exhibit an enhanced expression of activity-regulated cytoskeleton-associated protein (Arc) (17, 20–22), which has previously been shown to be reduced by comparable radiation exposures at relatively early post-irradiation time points (11, 20, 36, 37). Moreover, disruption of hippocampal neurogenesis has been directly implicated in impaired performance in the NOR paradigm, and has been correlated with impaired induction and maintenance of LTP (33, 38).

Alternatively, functional deficits produced by 10 Gy WBI may reflect a more generalized impairment of neuronal plasticity among mature neurons within the hippocampus and/or associated parahippocampal structures. Several reports have established that, in addition to the hippocampus, the perirhinal and insular cortices are also required for consolidation of NOR memory (39–42). Similarly, though the induction and maintenance of LTP by perforant pathway stimulation is unambiguously localized within the dentate gyrus, the associated up-regulation of activity-induced proteins occurs primarily among functionally mature neurons (18, 43). Thus, the deleterious effects of irradiation in this context may reflect neuroinflammation-induced suppression of processes related to activity-induced gene expression and/or the associated modifications of synaptic structure. Regardless of the

underlying mechanisms, however, these improvements in NOR consolidation and in LTP induction and maintenance suggests that the mitigating effects of MW-151 are sufficient to preserve/ restore the functional status of the hippocampal network to a near-normal state, even at very late time points post-WBI and long after therapy withdrawal.

It is apparent from these preliminary investigations that the selective and transient suppression of proinflammatory microglial cytokines postirradiation represents a promising mitigating therapy in this context. Ongoing investigations will expand upon these results and address several methodological deficiencies. Activity-induced increases in neurogenesis, neuronal survival and gene/protein expression within the hippocampus are necessary for optimal consolidation of spatial memory (36, 37, 44). Thus, future investigations will assess their relative contributions to the deficits associated with late radiation-induced cognitive impairment, in which their respective induction kinetics are examined in parallel and at post-irradiation time points that encompass the full range of neuronal maturation within the dentate gyrus and/or the evolution of radiation-induced functional deficits. These investigations will use a broader array of behavioral assays of spatial memory, both as inducers of hippocampal plasticity and as measures of memory consolidation. More comprehensive assays of neuroinflammation will also be incorporated to assess the relative roles of specific proinflammatory cytokines and chemokines in this context.

Acknowledgments

The authors wish to thank Lori Klamann, Ph.D., Bruce Connop, Ph.D., and Carl Diamani, Ph.D., of Transition Therapeutics, Toronto, Ontario, CA, for their assistance in establishing our MW-151 dilution and dose regimen. MW-151 was obtained by a Material Transfer Agreement with Transition Therapeutics. These studies were supported in part by a pilot project from the Center for Medical Countermeasures against Radiation injury (CMCR) sponsored by NIH/NIAID U19AI067734-049001 (PI: John E. Moulder, Ph.D.).

References

1. Abayomi OK. Pathogenesis of cognitive decline following therapeutic irradiation for head and neck tumors. *Acta Oncol.* 2002; 41:346–51. [PubMed: 12234025]
2. Butler JM, Rapp SR, Shaw EG. Managing the cognitive effects of brain tumor radiation therapy. *Curr Treat Options Oncol.* 2006; 7:517–23. [PubMed: 17032563]
3. Dropcho EJ. CNS injury by therapeutic irradiation. *Neurol Clin.* 1991; 9:969–88. [PubMed: 1758435]
4. Ghia A, Tome WA, Thomas S. Distribution of brain metastases in relation to the hippocampus: implications for neurocognitive function preservation. *Int J Radiat Oncol Biol Phys.* 2007; 68:971–7. [PubMed: 17446005]
5. Chang EL, Wefel JS, Hess KR, Allen PK, Lang FF, Kornguth DG, et al. Neurocognition in patients with brain metastases treated with radiosurgery or radiosurgery plus whole-brain irradiation: a randomized controlled trial. *Lancet Neurol.* 2009; 10:1037–44.
6. Douw L, Klein M, Fagle SSAA, van den Heuvel J, Taphoorn MJB, Aaronson NK, et al. Cognitive and radiological effects of radiotherapy in patients with low-grade glioma: long-term follow-up. *Lancet Neurol.* 2009; 8:810–8. [PubMed: 19665931]
7. Monje ML, Toda H, Palmer TD. Inflammatory blockade restores adult hippocampal neurogenesis. *Science.* 2003; 302:1760–5. [PubMed: 14615545]
8. Monje ML, Mizumatsu S, Fike JR, Palmer TD. Irradiation induced neural precursor-cell dysfunction. *Nature Med.* 2002; 8:955–62. [PubMed: 12161748]
9. Ekdahl CT, Claassen JH, Bonde S, Kokaia Z, Lindvall O. Inflammation is detrimental for neurogenesis in adult brain. *PNAS.* 2003; 100:13632–7. [PubMed: 14581618]
10. Raola R, Raber J, Rizk A, Otsuka S, VandenBerg SR, Morherdt DR, et al. Radiation-induced impairment of hippocampal neurogenesis is associated with cognitive deficits in young mice. *Exp Neurol.* 2004; 188:316–30. [PubMed: 15246832]

11. Rosi S, Andres-Mach M, Fishman KM, Levy W, Ferguson RA, Fike JR. Cranial irradiation alters the behaviorally induced immediate-early gene Arc (activity-regulated cytoskeleton-associated protein). *Cancer Res.* 2008; 68:9763–70. [PubMed: 19047155]
12. Rosi S, Ramirez-Amaya V, Vazdaranova A, Esparza EE, Larkin PB, Fike JR, et al. Accuracy of hippocampal network activity is disrupted by neuroinflammation: rescued by metamine. *Brain.* 2009; 132:2464–77. [PubMed: 19531533]
13. Burrell K, Hill RP, Zadeh G. High-resolution in vivo analysis of normal brain response to cranial irradiation. *PLoS One.* 2012; 7:e38366. [PubMed: 22675549]
14. Zhao W, Payne V, Tommasi E, Diz DI, Hsu FC, Robbins ME. Administration of the peroxisomal proliferation-activated receptor gamma agonist piolitzazone during fractionated brain irradiation prevents radiation-induced cognitive impairment. *Int J Radiat Oncol Biol Phys.* 2007; 67:6–9. [PubMed: 17189061]
15. Robbins ME, Payne V, Tommasi E, Diz DI, Hsu FC, Brown WR, et al. The AT1 receptor antagonist, L-158,809, prevents or ameliorates fractionated whole-brain irradiation-induced cognitive impairment. *Int J Radiat Oncol Biol Phys.* 2009; 73:499–505. [PubMed: 19084353]
16. Palmer TD, Willhoite AR, Gage FH. Vascular niche for adult hippocampal neurogenesis. *J Comp Neurol.* 2000; 425:479–94. [PubMed: 10975875]
17. Kitamura T, Saitoh Y, Takashima N, Murayama A, Niibori Y, Ageta H, et al. Adult neurogenesis modulates the hippocampus-dependent period of associative fear memory. *Cell.* 2009; 139:814–27. [PubMed: 19914173]
18. Kuipers SD, Tiron A, Soule J, Messaoudi E, Trentani A, Bramham CR. Selective survival and maturation of adult-born dentate granule cells expressing the immediate early gene Arc/Arg3.1. *PLoS One.* 2009; 4(3):e4885. [PubMed: 19290048]
19. Zhao C, Teng EM, Summers RG, Ming GL, Gage FH. Distinct morphological stages of dentate granule neuron maturation in the adult mouse hippocampus. *J Neurosci.* 2006; 26:3–11. [PubMed: 16399667]
20. Bramham CR, Alme MN, Bittins M, Kuipers SD, Nair RR, Pai B, et al. The Arc of synaptic memory. *Exp Brain Res.* 2010; 200:125–40. [PubMed: 19690847]
21. Ramirez-Amaya V, Marrone DF, Gage FH, Worley PF, Barnes CA. Integration of new neurons into functional neural networks. *J Neurosci.* 2006; 22:12237–41. [PubMed: 17122048]
22. Toni N, Laplagne DA, Zhao C, Lombardi G, Ribak CE, Gage FH, et al. Neurons born in the adult dentate gyrus form functional synapses with target cells. *Nature Neurosci.* 2008; 11:901–7. [PubMed: 18622400]
23. Somera-Molina KC, Robin B, Somera CA, Anderson C, Stine C, Koh S, et al. Glial activation links early-life seizures and long-term neurologic dysfunction: evidence using a small molecule inhibitor of proinflammatory cytokine upregulation. *Epilepsia.* 2007; 48:1785–800. [PubMed: 17521344]
24. Lloyd E, Somera-Molina K, Van Eldik LJ, Watterson M, Wainwright MS. Suppression of acute proinflammatory cytokine and chemokine upregulation by post-injury administration of a novel small molecule improves long-term neurologic outcome in a mouse model of traumatic brain injury. *J Neuroinflamm.* 2008; 30(5):28.
25. Bachstetter AD, Norris CM, Sompol PJ, Wilcock DM, Goulding D, Neltner JH, et al. Early stage drug treatment that normalizes proinflammatory cytokine production attenuates synaptic dysfunction in a mouse model that exhibits age-dependent progression of Alzheimer's disease-related pathology. *J Neurosci.* 2012; 32:10201–10. [PubMed: 22836255]
26. Jenrow KA, Brown SL, Liu J, Kolozsvary A, Lapanowski K, Kim JH. Ramipril mitigates radiation-induced impairment of neurogenesis in the rat dentate gyrus. *Rad Oncol.* 2010; 5:6.
27. Jenrow KA, Liu J, Brown SL, Kolozsvary A, Lapanowski K, Kim JH. Combined atorvastatin and ramipril mitigate radiation-induced impairment of dentate gyrus neurogenesis. *J Neurooncol.* 2011; 101:449–56. [PubMed: 20617366]
28. Burger PC, Shibata T, Kleihues P. The use of the monoclonal antibody Ki-67 in the identification of proliferating cells: Application to surgical neuropathology. *Am J Surg Pathol.* 1986; 10:611–7. [PubMed: 2428262]

29. Sarnat HB, Nochlin D, Born DE. Neuronal nuclear antigen (NeuN): a marker of neuronal maturation in the early human fetal nervous system. *Brain Dev.* 1998; 20:88–94. [PubMed: 9545178]
30. Rosi S, Ramirez-Amaya V, Vazdaranova A, Worley PF, Barnes CA, Wenk GL. Neuroinflammation alters the hippocampal pattern of behaviorally induced Arc expression. *J Neurosci.* 2005; 25:723–31. [PubMed: 15659610]
31. Mumby DG, Gaskin S, Glenn MJ, Schramek TE, Lehmann H. Hippocampal damage and exploratory preference in rats: memory for objects, places, and contexts. *Learn Memory.* 2002; 9:49–57.
32. Gilbert ME, Mack CM. Field potential recordings in dentate gyrus of anesthetized rats: stability of baseline. *Hippocampus.* 1999; 9:227–87.
33. Lonergan PE, Martin DSD, Horrobin DF, Lynch MA. Neuroprotective effect of eicosapentaenoic acid in hippocampus of rats exposed to γ -irradiation. *J Biol Chem.* 2002; 277:20804–11. [PubMed: 11912218]
34. Ge S, Yang CH, Hsu KS, Ming GL, Song H. A critical period for enhanced synaptic plasticity in newly generated neurons of the adult brain. *Neuron.* 2007; 54:559–66. [PubMed: 17521569]
35. Schmidt-Hieber C, Jonas P, Bischofberger J. Enhanced synaptic plasticity in newly generated granule cells of the adult hippocampus. *Nature.* 2004; 410:184–7. [PubMed: 15107864]
36. Guzowski JF, Lyford GL, Stevenson GD, Houston FP, McLaugh JL, Worley PF, et al. Inhibition of activity-dependent Arc protein expression in the rat hippocampus impairs the maintenance of long-term potentiation and the consolidation of long-term memory. *J Neurosci.* 2000; 20:3993–4001. [PubMed: 10818134]
37. Plath N, Ohana O, Dammermann B, Errington ML, Schmitz D, Gross C, et al. Arc/Arg3.1 is essential for the consolidation of synaptic plasticity and memories. *Neuron.* 2006; 52:436–44.
38. Jessberger S, Clark RE, Broadbent NJ, Clemenson GD, Consiglio A, Lie DC, et al. Dentate gyrus-specific knockdown of adult neurogenesis impairs spatial and object recognition memory in adult rats. *Learn Memory.* 2009; 16:147–54.
39. Balderas I, Rodriguez-Ortiz CJ, Salgado-Tonda P, Chavez-Hurtado J, McLaugh JL, Bermudez-Rattoni F. The consolidation of object and context recognition memory involve different regions of the temporal lobe. *Learn Memory.* 2008; 15:618–24.
40. Broadbent NJ, Gaskin S, Squire LR, Clark RE. Object recognition memory and the rodent hippocampus. *Learn Memory.* 2010; 17:5–11.
41. Broadbent NJ, Squire LR, Clark RE. Spatial memory, recognition memory and the hippocampus. *PNAS.* 2004; 101:14515–20. [PubMed: 15452348]
42. Winters BD, Saksida LM, Bussey TJ. Object recognition memory: neurobiological mechanisms of encoding, consolidation and retrieval. *Neurosci Biobehav Rev.* 2008; 32:1055–70. [PubMed: 18499253]
43. Rodriguez JJ, Davies HA, Silva AT, De Souza IEJ, Peddie CJ, Colyer FM, et al. Long-term potentiation in the rat dentate gyrus is associated with enhanced Arc/Arg3.1 protein expression in spines, dendrites and glia. *E J Neurosci.* 2005; 21:2384–96.
44. Clelland CD, Choi M, Romberg C, Clemenson GD, Fagniere A, Tyers P, et al. A functional role for adult hippocampal neurogenesis in spatial pattern recognition. *Science.* 2009; 325:210–3. [PubMed: 19590004]

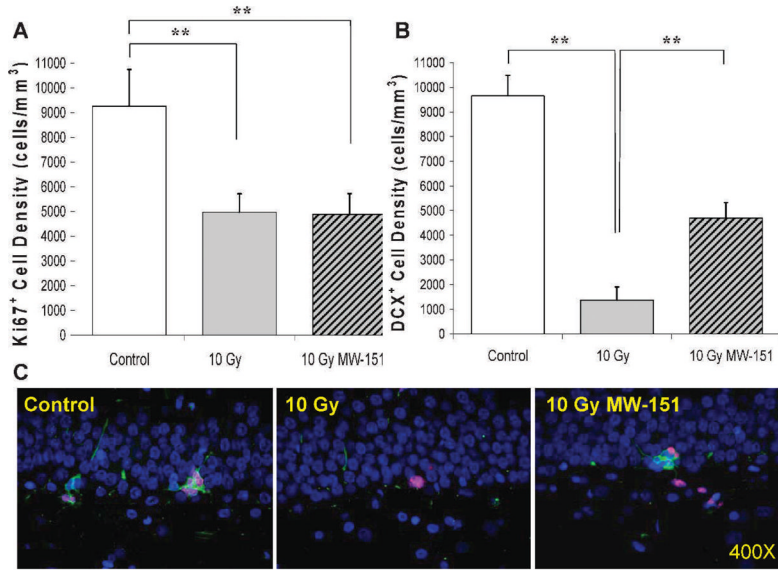
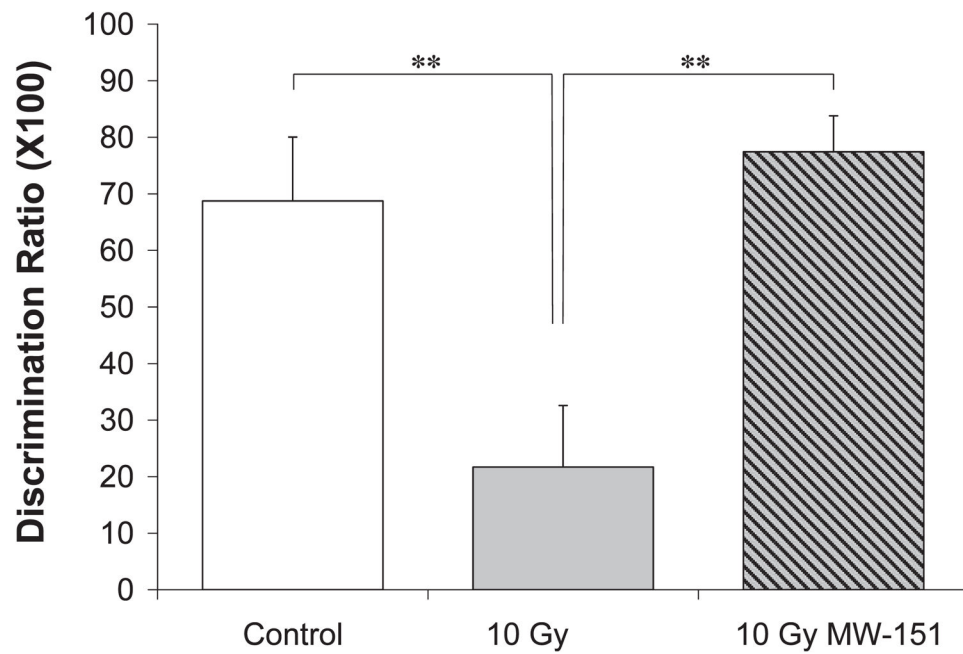
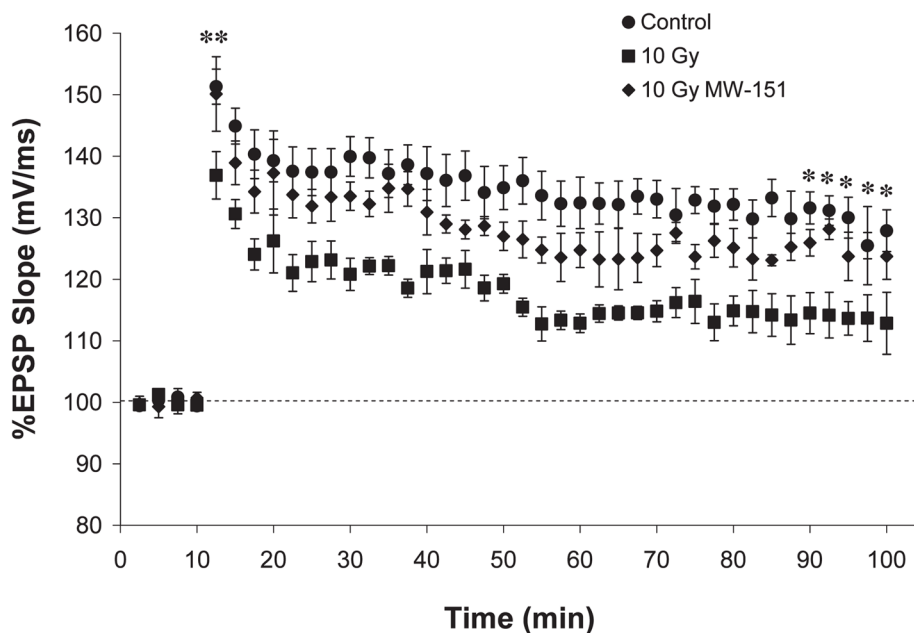


FIG. 1.

Counts of Ki67⁺ proliferating progenitors within the SGZ and DCX⁺ immature neurons within the SGZ and granule cell layer of the dentate gyrus were assayed at 2 months post-WBI at 0 (Control) or 10 Gy (10 Gy sham). Panel A: Relative to control, progenitor proliferation was significantly reduced in the 10 Gy (10 Gy sham) group (***P* < 0.01) and this reduction was not mitigated by MW-151 therapy in the 10 Gy MW-151 group (10 Gy MW-15). Panel B: Relative to control, neurogenesis was also significantly reduced (***P* < 0.01) in the 10 Gy group. However, MW-151 therapy produced significant mitigation (***P* < 0.01) with respect to neurogenesis (10 Gy MW-151). Panel C: Representative immunofluorescence images of Ki67⁺ (red) and DCX⁺ (green) cells in the SGZ of the dentate gyrus for control, 10 Gy and 10 Gy MW-151, using DAPI (blue) as a general label of cell nuclei (counterstain). The mitigating effects of MW-151 with respect to neurogenesis resulted in a higher proportion of Ki67⁺ cells in the 10 Gy MW-151 group differentiating into DCX⁺ immature neurons.

**FIG. 2.**

Novel Object Recognition (NOR) is a measure of hippocampal-dependent learning and memory function. Consolidation of memory for a previously encountered “familiar” object is revealed as an intrinsic bias for exploring a simultaneously-presented “novel” object, resulting in discrimination ratios > 0 . Relative to unirradiated controls (Control), discrimination ratios were significantly reduced ($**P < 0.01$) in the 10 Gy group when assayed 6 months postirradiation, indicating that 10 Gy WBI impairs the consolidation of recognition memory. MW-151 therapy, initiated 24 h postirradiation and maintained daily for 28 days, significantly mitigated ($**P < 0.01$) the deleterious effects of 10 Gy WBI on discrimination ratios (10 Gy MW-151).

**FIG. 3.**

Long-term potentiation (LTP) is a measure of synaptic plasticity that mimics the potentiation of synaptic function associated with hippocampal learning and memory. LTP is induced by a brief interval of high-frequency stimulation and is most reliably measured as an abrupt (induction) and sustained (maintenance) increase in the rising slope of the EPSP produced in response to individual test pulses. Relative to unirradiated controls (Control), EPSP slopes were significantly (** $P < 0.01$) reduced in the 10 Gy group when assayed 9 months postirradiation, indicating that 10 Gy WBI impairs both the induction and maintenance of LTP. Relative to 10 Gy, MW-151 mitigated both the induction (** $P < 0.01$) and maintenance ($*P < 0.03$) of LTP (10 Gy MW-151).

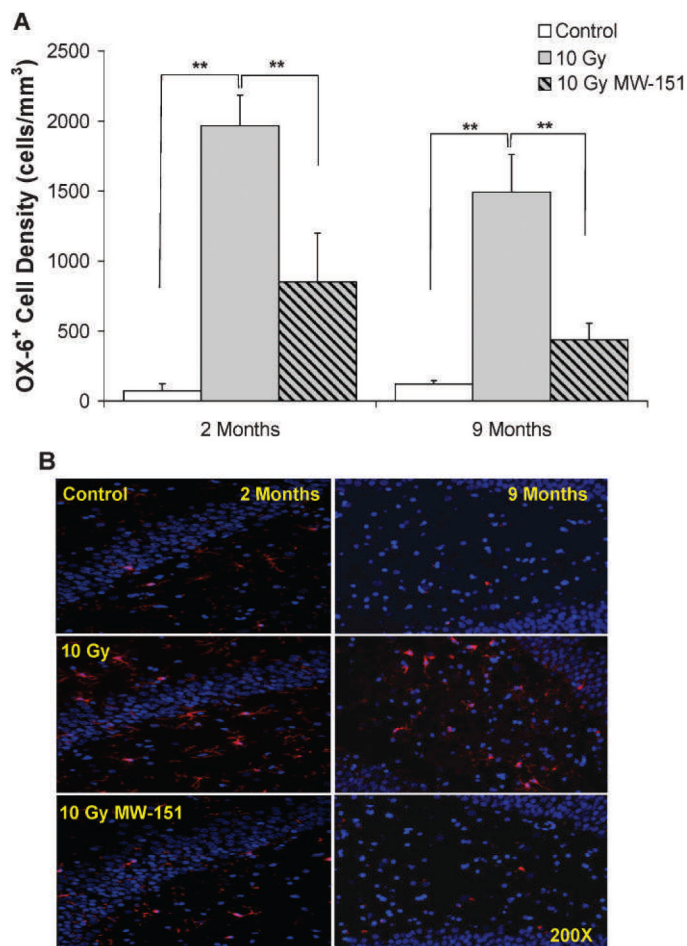


FIG. 4. Panel A: Average densities of OX-6⁺ activated microglia assayed at 2 and 9 months post-WBI in the rat dentate gyrus. Relative to unirradiated controls (Control), OX-6⁺ microglia are significantly increased (** $P < 0.01$) at both time points by 10 Gy WBI. However, these increases are significantly mitigated (** $P < 0.01$) by MW-151 (10 Gy MW-151). Panel B: Representative immunofluorescence images of OX-6⁺ activated microglia in the rat dentate gyrus at 2 and 9 months post-WBI using DAPI (blue) as a general label of cell nuclei (counterstain). Relative to control, OX-6⁺ activated microglia (red) are increased in 10 Gy consistent with chronic neuroinflammation.